

pubs.acs.org/NanoLett Letter

Lipid Phase Separation in Vesicles Enhances TRAIL-Mediated Cytotoxicity

Timothy Q. Vu, Justin A. Peruzzi, Lucas E. Sant'Anna, Eric W. Roth, and Neha P. Kamat*



Cite This: https://doi.org/10.1021/acs.nanolett.1c04365



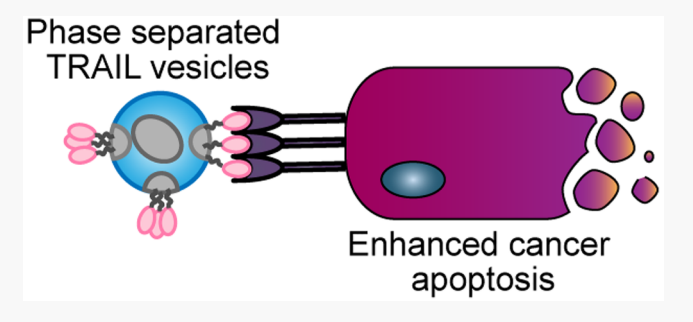
ACCESS

Metrics & More



s Supporting Information

ABSTRACT: Ligand spatial presentation and density play important roles in signaling pathways mediated by cell receptors and are critical parameters when designing protein-conjugated therapeutic nanoparticles. Here, we harness lipid phase separation to spatially control the protein presentation on lipid vesicles. We use this system to improve the cytotoxicity of TNF-related apoptosis inducing ligand (TRAIL), a therapeutic anticancer protein. Vesicles with phase-separated TRAIL presentation induce more cell death in Jurkat cancer cells than vesicles with uniformly presented TRAIL, and cytotoxicity is dependent on TRAIL density. We assess this relationship in other cancer cell lines and



demonstrate that phase-separated vesicles with TRAIL only enhance cytotoxicity through one TRAIL receptor, DR5, while another TRAIL receptor, DR4, is less sensitive to TRAIL density. This work demonstrates a rapid and accessible method to control protein conjugation and density on vesicles that can be adopted to other nanoparticle systems to improve receptor signaling by nanoparticles.

KEYWORDS: phase separation, Janus particles, vesicles, liposomes, TRAIL, lipid domains

he spatial presentation of ligands has a critical impact on cellular response. The density and interligand distance of extracellular ligands interacting with their receptors can control binding and adhesion, ultimately affecting cell signaling pathways and controlling a range of processes from immune responses to stem cell differentiation. 1-3 For ligand-conjugated, therapeutic nanoparticles, the ligand density and spacing can affect cellular binding and uptake and receptor activation. 4,5 By considering the role of ligand spatial presentation, therapeutic nanoparticles may be better designed to elicit desired cellular responses. Toward this goal, Janus nanoparticles, particles with two unique surfaces with distinct properties, have been developed to control the location and density of surface-conjugated ligands. Janus nanoparticles allow precise patterning of ligands on opposite faces, which have been used to study endocytosis of partial PEGylation⁶ and ligand clustering for T cell activation^{7,8} and to develop nanoparticles that mimic antibodies. Yet the assembly of these particles is difficult, requiring complex chemistry and manufacturing schemes, hindering their adoption as therapeutic nanoparticles despite their unique advantages.

In contrast to nanoparticles, cellular membranes naturally control the spatial presentation of ligands using phase-segregated lipid rafts. Lipid rafts are compartmentalized regions on the cell membrane characterized by increased cholesterol and saturated lipid content. These structures segregate distinct populations of biomolecules, affecting local membrane properties, lipid—protein interactions, and protein

signaling.¹⁰ Phase separation can be readily replicated in synthetic, self-assembled lipid systems.¹¹ Phospholipid bilayers, in both planar and nanoparticle form, can undergo phase separation when the appropriate mixtures of membrane components are used.^{12,13} Beyond a limited number of examples,^{14,15} this rich physical phenomenon has rarely been exploited to better design therapeutic nanoparticles.

A therapeutic target that could benefit from controlled presentation of ligands on a nanoparticle surface is the death receptor apoptosis pathway for anticancer therapy. In this pathway, TNF-related apoptosis inducing ligand (TRAIL), a homotrimer, binds to death receptors DR4 and DR5 upregulated in cancer cells and induces apoptosis. As TRAIL exhibits enhanced activity during oligomerization, recombinant TRAIL often requires further clustering or cross-linking for therapeutic use. For example, TRAIL signaling has been shown to improve when conjugated onto a lipid vesicle (liposome) compared to soluble TRAIL. This improvement is attributed to vesicle-promoted TRAIL oligomerization on the cell surface. Despite this improvement,

Received: November 11, 2021 Revised: February 1, 2022



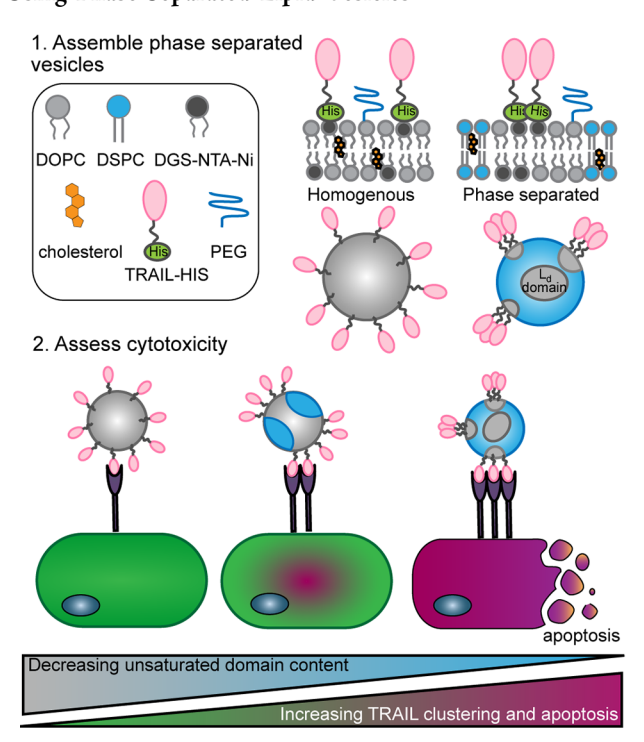
TRAIL-conjugated vesicles still perform poorly in vivo, in part because we do not fully understand how TRAIL density impacts signaling. Methods that allow for greater control of TRAIL presentation should allow us to study TRAIL signaling and improve the anticancer activity of TRAIL-conjugated therapeutic nanoparticles.

We set out to test whether we could control TRAIL density through changes in lipid composition in vesicles, and whether the density of TRAIL could improve signaling and cancer cell apoptosis. By conjugating TRAIL to unsaturated lipids and varying the concentration of domain-forming saturated lipids, we reasoned that we could control TRAIL density in vesicles by decreasing the surface area available to TRAIL-conjugated lipids while keeping the concentration of TRAIL per nanoparticle constant overall. Furthermore, we hypothesized that TRAIL localization would improve receptor oligomerization on target cells and TRAIL-mediated signaling would increase, ultimately enhancing apoptosis. Using recombinant TRAIL, we show the extent to which lipid phase separation can be harnessed to change the spatial density of TRAIL on vesicle surfaces and increase TRAIL signaling. By leveraging the intrinsic ability of lipid vesicles to phase separate, we demonstrate that lipid composition can be engineered to modulate the spatial density of proteins on a vesicle surface and promote TRAIL clustering and cytotoxic efficacy (Scheme

To control the surface density of TRAIL on liposomes, we assembled nanovesicles with varying levels of membrane phase separation. DOPC (1,2-dioleoyl-sn-glycero-3-phosphocholine), an unsaturated lipid, forms a liquid-disordered (L_d) phase, whereas DSPC (1,2-distearoyl-sn-glycero-3-phosphocholine)/ cholesterol mixtures form a liquid-ordered (L_o) phase.²¹ When mixed at appropriate ratios, these three lipids can phase separate into L_d and L_o phases within a single vesicle membrane. Lipid vesicles are assembled using ternary mixtures of DOPC and DSPC at varying ratios with cholesterol at a constant 30 mol %. To localize TRAIL to select regions of the membrane, we included an unsaturated lipid with a Ni-NTA (nickel-nitrilotriacetic acid) headgroup that localized into L_d regions in the liposome membrane. This Ni-NTA lipid allows conjugation of His-tagged TRAIL to our vesicles after vesicle formation. Polyethylene glycol (PEG, [18:0 PEG(2000)]), conjugated to a saturated lipid, was incorporated at 1 mol % for vesicle stability and should partition away from Ni-NTA lipids to reduce possible steric hindrance. Vesicles were extruded to 100 nm, an ideal size for drug delivery, incubated with His-tagged TRAIL, and dialyzed to remove unconjugated protein. By increasing the ratio of DSPC to DOPC in these vesicles, we expected to increase the size of Lo domains and reduce the size of L_d domains, respectively.

We used microscopy and Förster resonance energy transfer (FRET) analysis to confirm lipid phase separation. Vesicles are labeled with a saturated lipid dye (16:0 NBD, [N-(7-nitrobenz-2-oxa-1,3-diazol-4-yl)]) and an unsaturated lipid dye (18:1 Rho, [Lissamine-Rhodamine PE]) that should separate into L_o and L_d domains, respectively. Because we cannot visualize lipid domains in nanovesicles using microscopy, we created giant unilamellar vesicles (GUVs), micron-sized vesicles formed through electroformation with properties complementary to those of nanovesicles. ¹¹ GUVs showed segregation of 16:0 NBD and 18:1 Rho into distinct regions of the membrane in ternary compositions of DOPC, DSPC, and cholesterol, confirming the formation of phase-separated lipid domains

Scheme 1. Design of TRAIL-Conjugated Nanoparticles Using Phase-Separated Lipid Vesicles^a



"(Top) By varying the ratio of unsaturated lipid (DOPC), saturated lipid (DSPC), and cholesterol, lipid vesicles can be assembled containing homogenous or phase-segregated membranes. A nickel-conjugated lipid (DGS-NTA-Ni) that integrates into the liquid disordered phase of the membrane can bind histidine-tagged TRAIL proteins and generate nanoparticles with varying spatial densities of TRAIL. (Bottom) Nanoparticles with low unsaturated lipid content and increased density of TRAIL are hypothesized to enhance apoptosis in target cells.

(Figure 1a). In compositions with only DOPC or DSPC and cholesterol, the two dyes did not segregate. Next, we measured the FRET efficiency between 16:0 NBD (donor) and 18:1 Rho (acceptor) to assess the spatial separation between L₀ and L_d phases in nanovesicles that would be used for cell studies (Figure 1b).^{22,23} These studies demonstrated measurable differences in FRET ratio (here reported as normalized $F_{\rm donor}/F_{\rm acceptor}$ [see eqs 1 and 2 in Supporting Information] as a function of DSPC content, suggesting differences in phase separation as a function of vesicle composition (Figure 1c). As expected, vesicles composed of DOPC alone showed the lowest FRET ratio, indicating the two fluorescent probes were more uniformly distributed across the membrane. Increases in the mole fraction of DSPC increased the FRET ratio, indicating the saturated and unsaturated lipids were located farther apart within a given membrane and suggesting the presence of nanodomains. Pure DSPC vesicles exhibited the highest FRET ratio, which we attribute to the presence of extremely small L_d domains that result from segregation of the NTA-lipids and unsaturated lipid dye. Conjugation of TRAIL to DGS-NTA-Ni did not change vesicle FRET values, indicating the conjugation of TRAIL does not disrupt domains (Figure 1d). To further confirm that the FRET data reflect the presence of membrane domains, we used a temperature ramp to destabilize domains. 11,22 Our temperature studies show that the FRET ratio is temperature-dependent and decreased at

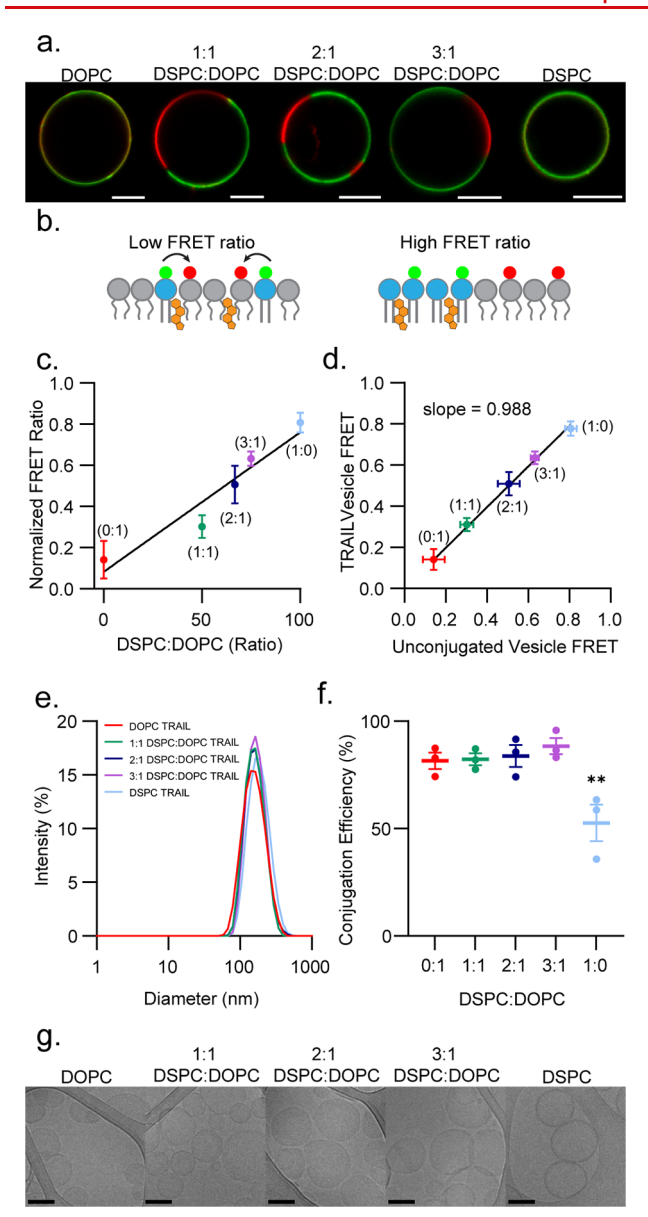


Figure 1. Characterization of TRAIL conjugation to lipid domain vesicles. (a) Microscopy images of GUVs show phase separation of saturated lipids (green) and unsaturated lipids (red). Scale bars are 10 μ m. (b) Schematic of a FRET assay to determine the lipid domain presence in vesicles. (c) FRET analysis of vesicle lipid domains before TRAIL conjugation, where the increasing FRET ratio indicates the presence of domains. The FRET ratio is reported as $F_{\rm donor}/F_{\rm acceptor}$. (d) FRET analysis of vesicle lipid domains before and after TRAIL conjugation shows no change after TRAIL conjugation. (e) Size distribution of TRAIL-conjugated vesicles measured by dynamic light scattering (DLS). (f) Conjugation efficiency of TRAIL to vesicles, as determined by Western blot. Results were analyzed by ANOVA compared to 0:1 DSPC:DOPC as a control. **** p < 0.0001, *** p < 0.00010.001, ** p < 0.01, * p < 0.05. (g) Cryo-electron microscopy images of TRAIL vesicles. Scale bar = 100 nm. Error bars represent SEM from n = 3 different vesicle preparations (panels c-f).

higher temperatures; this result is expected, as domains are known to dissolve and lipids become well mixed when the melting temperature ($T_{\rm m}$) of the saturated lipid is approached (55 °C for DSPC, Supporting Figure S1). In summary, our characterization of giant and nanosized vesicles confirms that our choice of lipid mixtures yields vesicles with varied degrees

of lipid segregation, which is conserved upon TRAIL conjugation.

Next, we measured several physical and chemical properties of the TRAIL-conjugated vesicles. All TRAIL-conjugated vesicle compositions exhibit a similar size and ζ potential (Figure 1e and Supporting Table S1). We next confirmed the extent of TRAIL conjugation onto the vesicles using Western blot analysis. DOPC, 1:1 DSPC:DOPC, 2:1 DSPC:DOPC, and 3:1 DSPC:DOPC compositions all show similar levels of TRAIL conjugation, while DSPC vesicles demonstrate less TRAIL conjugation (Figure 1f and Supporting Figure S2A). We hypothesize that TRAIL conjugation to DSPC vesicles is poor because DGS-NTA-Ni is unsaturated and assembles into extremely small L_d domains. As a result, steric hindrance from conjugated TRAIL molecules could prevent other TRAIL molecules from associating with unoccupied/unbound DGS-NTA-Ni. Nonreducing Western blot analysis revealed oligomeric TRAIL structures in vesicles that increase in number as the L₀ domain size decreases (Supporting Figure S2B). DSPC vesicles exhibit extremely large oligomers, which supports our hypothesis that TRAIL-conjugated lipids are highly segregated in this region and are likely to prevent other TRAIL molecules from binding to unbound DGS-NTA-Ni. Nonetheless, all other compositions showed similar levels of TRAIL conjugation. Finally, we imaged our nanovesicles using cryo-electron microscopy (cryo-EM) before and after TRAIL conjugation (Figure 1g and Supporting Figure S3) and observed no changes in morphology across all samples. We therefore established a series of membrane compositions that display differential phase separation but similar overall total TRAIL concentrations and morphologies, allowing us to isolate the role of TRAIL spatial density on cell cytotoxicity.

We then studied the capacity of TRAIL-conjugated vesicles to initiate TRAIL-mediated apoptosis. To measure cytotoxicity of TRAIL-conjugated vesicles, we chose to first study Jurkat cells, which are more sensitive to TRAIL-conjugated vesicles than soluble TRAIL alone. This feature suggests Jurkat cells may be responsive to further spatial localization of TRAIL molecules within membrane domains.²⁰ Jurkat cells were treated with increasing concentrations of either soluble TRAIL or TRAIL-conjugated vesicles for 24 h (Figure 2a). Despite DOPC TRAIL and soluble TRAIL possessing similar relative IC₅₀ values (29 and 25 ng/mL, respectively), DOPC TRAIL vesicles were more efficacious, reducing viability to approximately 25% while the effect of soluble TRAIL plateaued at 50% even at higher concentrations (Supporting Figure S4). Furthermore, we observed that segregation in vesicle domains increased the cytotoxicity of TRAIL and that cytotoxicity correlated with smaller domain size (3:1 DSPC:DOPC > 2:1 DSPC:DOPC > 1:1 DSPC:DOPC > DOPC). Decreasing the domain size increased both the efficacy, as domain-containing vesicles killed virtually all Jurkat cells at 200 ng/mL, and potency (relative IC₅₀ of 17 ng/mL for 1:1 DSPC:DOPC, 7 ng/mL for 2:1 DSPC:DOPC, and 6 ng/mL for 3:1 DSPC:DOPC) of TRAIL-conjugated vesicles. Surprisingly, DSPC vesicles did not exhibit any significant TRAIL-mediated cytotoxicity. While DSPC TRAIL vesicles had significantly less TRAIL conjugated on their surface, the concentration of TRAIL on DSPC vesicles should still have been sufficient to induce apoptosis; therefore, some other feature of TRAIL presentation in these particles was likely affecting their efficacy. To rule out the possibility that the cytotoxic effects we observed were due to the lipid vesicles themselves, we treated

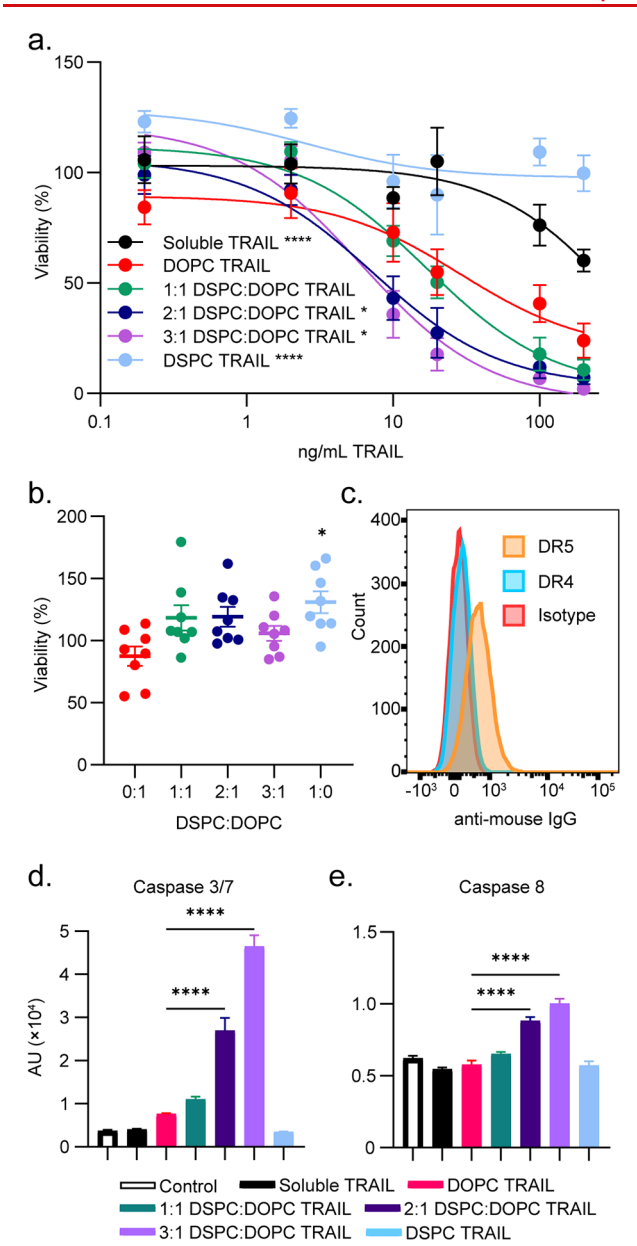


Figure 2. Vesicle lipid domains enhance TRAIL activation in Jurkat cells. (a) Viability of Jurkat cells treated with different concentrations of soluble and vesicle TRAIL after 24 h. Error bars represent SEM from n = 6 using two different vesicle preparations. The concentration reported is the initial amount of TRAIL added to the vesicles during conjugation. Results are analyzed by two-way ANOVA with multiple comparisons compared to DOPC TRAIL. (b) Viability of Jurkat cells to 1 mM unconjugated lipid vesicles, which corresponds to the highest TRAIL-conjugated vesicle concentration tested. Error bars represent SEM from n = 8 from three different vesicle preparations. pvalues reflect an ANOVA with multiple comparisons compared to untreated Jurkat cells. (c) Flow cytometry analysis of Jurkat expression of TRAIL receptors DR4 and DR5. (d, e) Activation of caspase 3/7 (d) and caspase 8 (e) in Jurkat cells exposed to soluble and vesicle TRAIL (20 nM) after 3 h. Error bars represent SEM from n = 3. p values are generated using ANOVA with multiple comparisons. **** p < 0.0001, *** p < 0.001, ** p < 0.01, * p < 0.05.

Jurkat cells with unconjugated vesicles at the highest lipid concentration (1 mM lipid) used (Figure 2b). As expected, Jurkat viability was not negatively affected by unconjugated vesicles. Flow cytometry analysis of TRAIL receptors showed

Jurkat cells express higher levels of DR5 relative to DR4 (Figure 2c). Binding studies of the vesicles to Jurkat cells demonstrated that increasing DSPC vesicle concentration increases the binding of vesicles to cells nonspecifically and that binding does not fully correlate with TRAIL-mediated cytotoxicity (Supporting Figures S5 and S6). We hypothesize that the reduced cytotoxicity of DSPC-TRAIL vesicles may be due to the increased rigidity of DSPC vesicles or an altered presentation of TRAIL molecules on the surface of DSPC vesicles. This is supported by previous studies that demonstrate membrane fluidity affected immunoliposome binding toward target cells. 24,25 Our other vesicle compositions that showed robust TRAIL activity contained more unsaturated lipids and correspondingly more fluid membranes. Altogether, these results indicate that clustering TRAIL within L_d domains of lipid vesicles increases cell signaling and apoptosis.

To further confirm TRAIL-mediated cell death, we next investigated the activation of intracellular apoptotic signaling molecules by monitoring caspase-3/7 and caspase-8 activity. When TRAIL binds to its receptors, death receptors 4 and 5 (DR4, DR5), it recruits FAS-associated protein with death domain (FADD) and pro-caspase-8 to the cell membrane. This leads to caspase-8 activation and subsequent caspase-3 and caspase-7 activation to induce apoptosis.²⁶ We therefore measured caspase-3/7 and caspase-8 activity to confirm cell death is the result of TRAIL-induced intracellular signaling. We measured caspase-3/7 and caspase 8 activity in Jurkat cells after 3 h of incubation with vesicles containing 20 ng/mL of TRAIL (Figure 2d,e, respectively). At this time point and concentration we saw minimal caspase activity from soluble TRAIL, DOPC TRAIL, 1:1 DSPC:DOPC TRAIL, or DSPC TRAIL, but vesicles with smaller domains in the 2:1 DSPC:DOPC TRAIL and 3:1 DSPC:DOPC TRAIL compositions showed significantly increased caspase activity. Therefore, segregation of TRAIL in the L_d domain of vesicles increased caspase 3/7 and caspase 8 activity after 3 h over DOPC vesicles presenting uniformly distributed TRAIL. Curiously, DOPC TRAIL did not show any differences in caspase activity relative to soluble TRAIL at this time point despite increased cytotoxic activity over soluble TRAIL after 24 h, which could indicate that clustering also affects the rate of caspase activity. Work studying Fas/FasL, which induces apoptosis similarly to TRAIL/DR5, demonstrated the ligand spacing of FasL affected the apoptosis rate, which could explain increased caspase activity in the phase-segregated 2:1 and 3:1 DSPC:DOPC TRAIL compositions but not DOPC TRAIL.²⁷ These results confirm the mode of TRAIL-vesicle mediated cytotoxicity is through caspase-mediated apoptosis and that concentrating TRAIL into vesicle membrane domains increases caspase activity.

Finally, we wanted to assess the reproducibility of our system with other cell types. We assessed the cytotoxicity of phase-segregated TRAIL vesicles on five additional cancer cell lines: U2-OS, U937, MDA-MB-231, K562, and HCT-116 (Figure 3a—e). Interestingly, we found that TRAIL segregation in membrane domains did not universally improve TRAIL cytotoxicity. Some cell types were sensitive to TRAIL segregation in domains similar to Jurkat cells (U2-OS, U937), while other cell types showed no differences in viability between soluble TRAIL or domain-segregated TRAIL (K562, KDA-MB-231, and HCT-116). Again, treatment of cells with unconjugated vesicles at the highest lipid

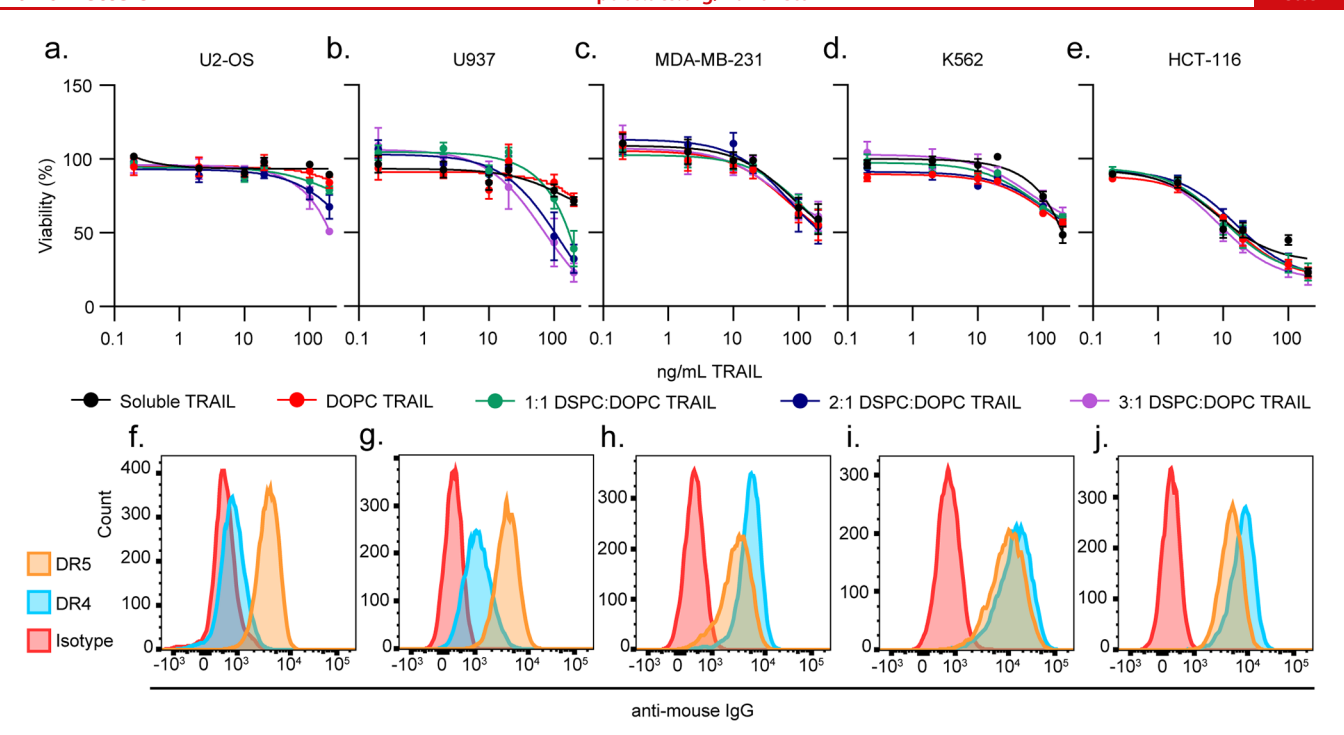


Figure 3. Cytotoxicity of TRAIL conjugated to vesicles with lipid domains depends on the cell type. Cell viability upon treatment with soluble and vesicle TRAIL after 24 h and expression of TRAIL receptors DR4/DR5 of U2-OS (a, f), U937 (b, g), MDA-MB-231 (c, h), K562 (d, i), and HCT-116 (e, j). Error bars represent SEM from n = 6 from two different vesicle preparations. The concentration reported is the initial amount of TRAIL added to the vesicles during conjugation. Only the 2:1 (*) and 3:1 (*) DSPC:DOPC TRAIL condition is statistically different from DOPC TRAIL for U2-OS and only the 3:1 DSPC:DOPC TRAIL condition is statistically different from DOPC TRAIL for U937 (*). Results are analyzed by two-way ANOVA with multiple comparisons compared to DOPC TRAIL as our control. * p < 0.05.

concentration showed no effects on viability, suggesting all observed cell death was dependent on TRAIL interactions with cells (Supporting Figure S7). DSPC TRAIL vesicles again showed limited cytotoxicity (Supporting Figure S8). We further tested caspase activity in U937 cells, one of the cells affected by TRAIL segregation in domains, and saw similar trends to what was observed in Jurkat cells (Supporting Figure S9). These results indicate that the capacity of spatial segregation to improve TRAIL mediated cell death is dependent on cell type.

We hypothesized that vesicle interactions with TRAIL receptors DR4 and DR5 may play a role in TRAIL sensitivity. Using flow cytometry, we measured the expression levels of DR4 and DR5 for each cell type (Figure 3f–j). We compared the DR5/DR4 expression level to the difference in cell viability between cells incubated with 3:1 DSPC:DOPC (phase segregated) or DOPC (uniform) TRAIL vesicles and identified two distinct clusters (Figure 4). Cells that predominantly expressed DR5 over DR4 were sensitive to TRAIL segregation in vesicle domains, while cells that expressed more or equivalent amounts of DR4 over DR5 showed no viability differences as a function of vesicle composition.

Previous studies have shown that DR5 and DR4 can respond differentially to TRAIL. DR5 benefits from TRAIL oligomerization in order to activate apoptotic signaling. ^{28–30} In contrast, TRAIL oligomerization has less of an effect on DR4 activation. ^{28,31,32} DR4 resides in lipid rafts in certain cell types that are susceptible to TRAIL, rendering TRAIL oligomerization unnecessary because DR4 is likely already preorganized. ³³ Because DR4 can competitively bind TRAIL from DR5, ^{31,34,35} the relative differences in receptor expression should dictate the extent to which TRAIL density influences

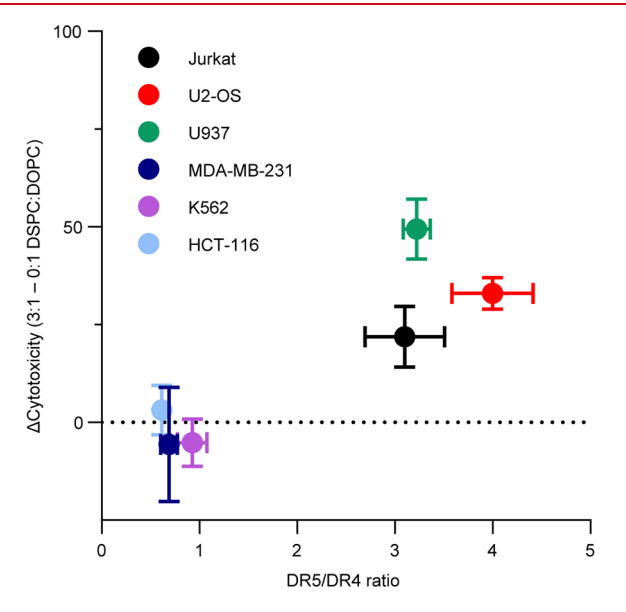


Figure 4. Enhancement of TRAIL cytotoxicity with lipid domains is dependent on DR4 and DR5 expression levels in target cells. The DR5/DR4 ratio on target cells is shown relative to the resulting cytotoxicity difference between 3:1 DSPC:DOPC TRAIL vesicles and pure DOPC TRAIL vesicles. Cytotoxicity differences between vesicles containing domains and homogeneous DOPC vesicles are only seen when DR5 is expressed higher than DR4. The error bar represents the SEM from n = 6 (y-axis) and n = 3 (x-axis).

apoptotic signaling. We expect, therefore, that when DR5 is more prevalent on cell membranes than DR4, TRAIL density should become more important, and vesicles that localize TRAIL in phase-segregated domains should affect the extent of

apoptotic signaling. In contrast, when DR4 is more prevalent and TRAIL signaling occurs primarily through this receptor, the spatial density of TRAIL should be less important, which we have observed in our studies. DR4 and DR5 can also form heterocomplexes, which is not well understood but has been shown to predominantly signal through DR4 in pancreatic tumor cells. Ultimately, the relative levels of DR4 and DR5 expression, and which receptor the cell predominantly signals through, could affect the therapeutic strategy for TRAIL agonists.

Lipid domains provide a straightforward route to control the spatial density of a lipid-linked protein to signal clusterdependent receptors like DR5. Our observations of TRAIL mediated cytotoxicity in cell types that express higher levels of DR5 relative to DR4 show that concentrating TRAIL in smaller lipid domains enhances cytotoxicity relative to vesicles with homogeneously distributed TRAIL. This observation is consistent with recent studies using DNA origami nanostructures: ligand spatial orientation improved apoptosis signaling in DR5 and Fas (CD95, a protein similar to DR5), with the optimal interligand distance at approximately 10 nm.^{27,38} We do note that increasing vesicle binding to cells through TRAIL domains (Figure S5) could have an effect on TRAIL cytotoxicity but does not fully explain cytotoxicity differences because DSPC vesicles bind strongest without corresponding increases in cytotoxicity. We therefore hypothesize that controlling TRAIL spatial orientation on lipid vesicles by using lipid domains most likely increases DR5-mediated apoptosis by approaching this critical interligand distance. Further studies to characterize lipid domains in nanovesicles, however, will be required to more widely adopt this method. The domain size and number on lipid vesicles is dynamic and widely distributed similarly to lipid rafts in cell membranes, and characterizing domains is extremely difficult.³⁹ Advances in cryo-EM have been developed to visualize lipid domains and protein localization in nanovesicles, which could allow us to better characterize how domain number and size could affect signaling.40,41

Vesicle phase separation is a useful technique to enhance protein-conjugated vesicles. Including optimization of TRAIL density for other TRAIL nanoparticle approaches could enhance TRAIL therapeutics in vivo. 26,42-46 From a biomaterials perspective, controlled spatial conjugation of proteins can apply to other types of vesicles with demonstrated phase separation, such as lipid-polymer hybrid vesicles^{23,47} and polymersomes, 48,49 as well as in supported bilayer systems and nanoparticles for fundamental investigations into the effects of spatial arrangements on biological mechanisms. 50,51 Biological systems that are also known to be dependent on receptor clustering include immune signaling receptors^{52,53} and receptor internalization. 54,55 Altogether, phase separated vesicles provide researchers a new tool to spatially control protein spacing for designing cell-mimetic systems and therapeutic nanoparticles.

ASSOCIATED CONTENT

Supporting Information

The Supporting Information is available free of charge at https://pubs.acs.org/doi/10.1021/acs.nanolett.1c04365.

Experimental section, and vesicle characterization, including FRET ratio changes over time (Figure S1), size and ζ potential of vesicles (Table S1), Western blot

of TRAIL conjugation (Figure S2), cryo-EM of unconjugated vesicles (Figure S3), additional TRAIL studies including more soluble TRAIL characterization (Figure S4), binding of TRAIL vesicles to Jurkats (Figure S5), microscopy of TRAIL vesicle binding to Jurkat cells (Figure S6), viability of cell line panel to unconjugated vesicles (Figure S7), DSPC TRAIL viability to cell line panel (Figure S8), caspase 3/7 and 8 data for U937 (Figure S9), and nanoparticle tracking analysis data to further characterize vesicles (Table S2) (PDF)

AUTHOR INFORMATION

Corresponding Author

Neha P. Kamat — Department of Biomedical Engineering, McCormick School of Engineering and Center for Synthetic Biology, McCormick School of Engineering, Northwestern University, Evanston, Illinois 60208, United States;

orcid.org/0000-0001-9362-6106; Email: nkamat@northwestern.edu

Authors

Timothy Q. Vu — Department of Biomedical Engineering, McCormick School of Engineering, Northwestern University, Evanston, Illinois 60208, United States

Justin A. Peruzzi — Department of Chemical and Biological Engineering, McCormick School of Engineering, Northwestern University, Evanston, Illinois 60208, United States

Lucas E. Sant'Anna — Department of Biomedical Engineering, McCormick School of Engineering, Northwestern University, Evanston, Illinois 60208, United States

Eric W. Roth — Northwestern University Atomic and Nanoscale Characterization and Experimentation Center, Northwestern University, Evanston, Illinois 60208, United States

Complete contact information is available at: https://pubs.acs.org/10.1021/acs.nanolett.1c04365

Author Contributions

T.Q.V., J.A.P., and N.P.K. conceived the study and designed experiments. T.Q.V., J.A.P., L.E.S, and E.W.R. performed the experiments, T.Q.V., J.A.P., and N.P.K. analyzed the data. All the authors contributed to writing the manuscript.

Notes

The authors declare the following competing financial interest(s): N.P.K, J.A.P, and T.Q.V. are inventors on a provisional patent filing related to the technology described here.

ACKNOWLEDGMENTS

This work was supported in part by the Searle Funds at The Chicago Community Trust and the National Science Foundation under Grant Nos. 1844219 and 1844336. T.Q.V. was supported by the National Institutes of Health Training Grant (T32GM008449) through Northwestern University's Biotechnology Training Program. J.A.P. gratefully acknowledges support from the Ryan Fellowship and the International Institute for Nanotechnology at Northwestern University. J.A.P. was supported by an NSF Graduate Research Fellowship. This work made use of the Northwestern RHLCCC Flow Cytometry Facility (NCI CA060553) and Northwestern NUANCE center (NSF ECCS-2025633 and NSF DMR-

1720139). This work made use of the BioCryo facility of Northwestern University's NUANCE Center, which has received support from the SHyNE Resource (NSF ECCS-2025633), the IIN, and Northwestern's MRSEC program (NSF DMR-1720139). We thank the Kamat lab members for careful reading of the manuscript and the Mrksich group for helpful discussions.

REFERENCES

- (1) Ye, K.; Wang, X.; Cao, L.; Li, S.; Li, Z.; Yu, L.; Ding, J. Matrix Stiffness and Nanoscale Spatial Organization of Cell-Adhesive Ligands Direct Stem Cell Fate. *Nano Lett.* **2015**, *15*, 4720–4729.
- (2) Chen, Z.; Wholey, W.-Y.; Hassani Najafabadi, A.; Moon, J. J.; Grigorova, I.; Chackerian, B.; Cheng, W. Self-Antigens Displayed on Liposomal Nanoparticles above a Threshold of Epitope Density Elicit Class-Switched Autoreactive Antibodies Independent of T Cell Help. *J. Immunol* **2020**, *204*, 335–347.
- (3) Smith, M. R.; Tolbert, S. V.; Wen, F. Protein-Scaffold Directed Nanoscale Assembly of T Cell Ligands: Artificial Antigen Presentation with Defined Valency, Density, and Ratio. *ACS Synth. Biol.* **2018**, *7*, 1629–1639.
- (4) Reuter, K. G.; Perry, J. L.; Kim, D.; Luft, J. C.; Liu, R.; DeSimone, J. M. Targeted PRINT Hydrogels: The Role of Nanoparticle Size and Ligand Density on Cell Association, Biodistribution, and Tumor Accumulation. *Nano Lett.* **2015**, *15*, 6371–6378.
- (5) Zhang, Q.; Reinhard, B. M. Ligand Density and Nanoparticle Clustering Cooperate in the Multivalent Amplification of Epidermal Growth Factor Receptor Activation. *ACS Nano* **2018**, *12*, 10473–10485.
- (6) Sanchez, L.; Yi, Y.; Yu, Y. Effect of Partial PEGylation on Particle Uptake by Macrophages. *Nanoscale* **2017**, *9*, 288–297.
- (7) Lee, K.; Yu, Y. Janus Nanoparticles for T Cell Activation: Clustering Ligands to Enhance Stimulation. *J. Mater. Chem. B* **2017**, *5*, 4410–4415.
- (8) Chen, B.; Jia, Y.; Gao, Y.; Sanchez, L.; Anthony, S. M.; Yu, Y. Janus Particles as Artificial Antigen-Presenting Cells for T Cell Activation. ACS Appl. Mater. Interfaces 2014, 6, 18435—18439.
- (9) Liu, J.; Toy, R.; Vantucci, C.; Pradhan, P.; Zhang, Z.; Kuo, K. M.; Kubelick, K. P.; Huo, D.; Wen, J.; Kim, J.; Lyu, Z.; Dhal, S.; Atalis, A.; Ghosh-Choudhary, S. K.; Devereaux, E. J.; Gumbart, J. C.; Xia, Y.; Emelianov, S. Y.; Willett, N. J.; Roy, K. Bifunctional Janus Particles as Multivalent Synthetic Nanoparticle Antibodies (SNAbs) for Selective Depletion of Target Cells. *Nano Lett.* **2021**, *21*, 875.
- (10) Sezgin, E.; Levental, I.; Mayor, S.; Eggeling, C. The Mystery of Membrane Organization: Composition, Regulation and Roles of Lipid Rafts. *Nat. Rev. Mol. Cell Biol.* **2017**, *18*, 361–374.
- (11) Veatch, S. L.; Keller, S. L. Separation of Liquid Phases in Giant Vesicles of Ternary Mixtures of Phospholipids and Cholesterol. *Biophys. J.* **2003**, *85*, 3074–3083.
- (12) Rideau, E.; Dimova, R.; Schwille, P.; Wurm, F. R.; Landfester, K. Liposomes and Polymersomes: A Comparative Review towards Cell Mimicking. *Chem. Soc. Rev.* **2018**, 47, 8572–8610.
- (13) Elson, E. L.; Fried, E.; Dolbow, J. E.; Genin, G. M. Phase Separation in Biological Membranes: Integration of Theory and Experiment. *Annu. Rev. Biophys.* **2010**, *39*, 207–226.
- (14) Imam, Z. I.; Kenyon, L. E.; Ashby, G.; Nagib, F.; Mendicino, M.; Zhao, C.; Gadok, A. K.; Stachowiak, J. C. Phase-Separated Liposomes Enhance the Efficiency of Macromolecular Delivery to the Cellular Cytoplasm. *Cell. Mol. Bioeng.* **2017**, *10*, 387–403.
- (15) Trementozzi, A. N.; Imam, Z. I.; Mendicino, M.; Hayden, C. C.; Stachowiak, J. C. Liposome-Mediated Chemotherapeutic Delivery Is Synergistically Enhanced by Ternary Lipid Compositions and Cationic Lipids. *Langmuir* **2019**, *35*, 12532.
- (16) von Karstedt, S.; Montinaro, A.; Walczak, H. Exploring the TRAILs Less Travelled: TRAIL in Cancer Biology and Therapy. *Nat. Rev. Cancer* **2017**, *17*, 352–366.

- (17) Spitzer, D.; McDunn, J. E.; Plambeck-Suess, S.; Goedegebuure, P. S.; Hotchkiss, R. S.; Hawkins, W. G. A Genetically Encoded Multifunctional Trail Trimer Facilitates Cell-Specific Targeting and Tumor Cell Killing. *Mol. Cancer Ther.* **2010**, *9*, 2142–2151.
- (18) De Miguel, D.; Gallego-Lleyda, A.; Ayuso, J. M.; Pejenaute-Ochoa, D.; Jarauta, V.; Marzo, I.; Fernández, L. J.; Ochoa, I.; Conde, B.; Anel, A.; Martinez-Lostao, L. High-Order TRAIL Oligomer Formation in TRAIL-Coated Lipid Nanoparticles Enhances DR5 Cross-Linking and Increases Antitumour Effect against Colon Cancer. *Cancer Lett.* **2016**, 383, 250–260.
- (19) Nair, P. M.; Flores, H.; Gogineni, A.; Marsters, S.; Lawrence, D. A.; Kelley, R. F.; Ngu, H.; Sagolla, M.; Komuves, L.; Bourgon, R.; Settleman, J.; Ashkenazi, A. Enhancing the Antitumor Efficacy of a Cell-Surface Death Ligand by Covalent Membrane Display. *Proc. Natl. Acad. Sci. U. S. A.* **2015**, *112*, 5679–5684.
- (20) De Miguel, D.; Gallego-Lleyda, A.; Anel, A.; Martinez-Lostao, L. Liposome-Bound TRAIL Induces Superior DR5 Clustering and Enhanced DISC Recruitment in Histiocytic Lymphoma U937 Cells. *Leuk. Res.* **2015**, *39*, 657–666.
- (21) Zhao, J.; Wu, J.; Heberle, F. A.; Mills, T. T.; Klawitter, P.; Huang, G.; Costanza, G.; Feigenson, G. W. Phase Studies of Model Biomembranes: Complex Behavior of DSPC/DOPC/Cholesterol. *Biochim. Biophys. Acta Biomembr.* **2007**, *1768*, 2764–2776.
- (22) Shishina, A. K.; Kovrigina, E. A.; Galiakhmetov, A. R.; Rathore, R.; Kovrigin, E. L. Study of Förster Resonance Energy Transfer to Lipid Domain Markers Ascertains Partitioning of Semisynthetic Lipidated N-Ras in Lipid Raft Nanodomains. *Biochemistry* **2018**, *57*, 872–881.
- (23) Dao, T. P. T.; Fernandes, F.; Er-Rafik, M.; Salva, R.; Schmutz, M.; Brûlet, A.; Prieto, M.; Sandre, O.; Le Meins, J. F. Phase Separation and Nanodomain Formation in Hybrid Polymer/Lipid Vesicles. *ACS Macro Lett.* **2015**, *4*, 182–186.
- (24) Almeda, D.; Wang, B.; Auguste, D. T. Minimizing Antibody Surface Density on Liposomes While Sustaining Cytokine-Activated EC Targeting. *Biomaterials* **2015**, *41*, 37–44.
- (25) Gunawan, R. C.; Auguste, D. T. The Role of Antibody Synergy and Membrane Fluidity in the Vascular Targeting of Immunoliposomes. *Biomaterials* **2010**, *31*, 900–907.
- (26) Le, D. H. T.; Commandeur, U.; Steinmetz, N. F. Presentation and Delivery of Tumor Necrosis Factor-Related Apoptosis-Inducing Ligand via Elongated Plant Viral Nanoparticle Enhances Antitumor Efficacy. ACS Nano 2019, 13, 2501.
- (27) Berger, R. M. L.; Weck, J. M.; Kempe, S. M.; Hill, O.; Liedl, T.; Rädler, J. O.; Monzel, C.; Heuer-Jungemann, A. Nanoscale FasL Organization on DNA Origami to Decipher Apoptosis Signal Activation in Cells. *Small* **2021**, *17*, 2101678.
- (28) Natoni, A.; MacFarlane, M.; Inoue, S.; Walewska, R.; Majid, A.; Knee, D.; Stover, D. R.; Dyer, M. J. S.; Cohen, G. M. TRAIL Signals to Apoptosis in Chronic Lymphocytic Leukaemia Cells Primarily through TRAIL-R1 Whereas Cross-Linked Agonistic TRAIL-R2 Antibodies Facilitate Signalling via TRAIL-R2. *Br. J. Hamaetol.* **2007**, *139*, 568–577.
- (29) Berg, D.; Stühmer, T.; Siegmund, D.; Müller, N.; Giner, T.; Dittrich-Breiholz, O.; Kracht, M.; Bargou, R.; Wajant, H. Oligomerized Tumor Necrosis Factor-Related Apoptosis Inducing Ligand Strongly Induces Cell Death in Myeloma Cells, but Also Activates Proinflammatory Signaling Pathways. FEBS J. 2009, 276, 6912–6927.
- (30) Beyrath, J.; Chekkat, N.; Smulski, C. R.; Lombardo, C. M.; Lechner, M.-C.; Seguin, C.; Decossas, M.; Spanedda, M. V.; Frisch, B.; Guichard, G.; Fournel, S.; Beyrath, J.; Chekkat, N.; Smulski, C. R.; Lombardo, C. M.; Lechner, M.-C.; Seguin, C.; Decossas, M.; Spanedda, M. V.; Frisch, B.; Guichard, G.; Fournel, S. Synthetic Ligands of Death Receptor 5 Display a Cell-Selective Agonistic Effect at Different Oligomerization Levels. *Oncotarget* **2016**, *7*, 64942–64956.
- (31) Kelley, R. F.; Totpal, K.; Lindstrom, S. H.; Mathieu, M.; Billeci, K.; DeForge, L.; Pai, R.; Hymowitz, S. G.; Ashkenazi, A. Receptor-Selective Mutants of Apoptosis-Inducing Ligand 2/Tumor Necrosis

- Factor-Related Apoptosis-Inducing Ligand Reveal a Greater Contribution of Death Receptor (DR) 5 than DR4 to Apoptosis Signaling. *J. Biol. Chem.* **2005**, 280, 2205–2212.
- (32) Wajant, H.; Moosmayer, D.; Wüest, T.; Bartke, T.; Gerlach, E.; Schönherr, U.; Peters, N.; Scheurich, P.; Pfizenmaier, K. Differential Activation of TRAIL-R1 and -2 by Soluble and Membrane TRAIL Allows Selective Surface Antigen-Directed Activation of TRAIL-R2 by a Soluble TRAIL Derivative. *Oncogene* **2001**, *20*, 4101–4106.
- (33) Marconi, M.; Ascione, B.; Čiarlo, L.; Vona, R.; Garofalo, T.; Sorice, M.; Gianni, A. M.; Locatelli, S. L.; Carlo-Stella, C.; Malorni, W.; Matarrese, P. Constitutive Localization of DR4 in Lipid Rafts Is Mandatory for TRAIL-Induced Apoptosis in B-Cell Hematologic Malignancies. *Cell Death Dis* **2013**, *4*, e863—e863.
- (34) Reis, C. R.; van der Sloot, A. M.; Natoni, A.; Szegezdi, E.; Setroikromo, R.; Meijer, M.; Sjollema, K.; Stricher, F.; Cool, R. H.; Samali, A.; Serrano, L.; Quax, W. J. Rapid and Efficient Cancer Cell Killing Mediated by High-Affinity Death Receptor Homotrimerizing TRAIL Variants. *Cell Death Dis* **2010**, *1*, e83–e83.
- (35) Bin, L.; Thorburn, J.; Thomas, L. R.; Clark, P. E.; Humphreys, R.; Thorburn, A. Tumor-Derived Mutations in the TRAIL Receptor DR5 Inhibit TRAIL Signaling through the DR4 Receptor by Competing for Ligand Binding. *J. Biol. Chem.* **2007**, 282, 28189–28194.
- (36) Lemke, J.; Noack, A.; Adam, D.; Tchikov, V.; Bertsch, U.; Röder, C.; Schütze, S.; Wajant, H.; Kalthoff, H.; Trauzold, A. TRAIL Signaling Is Mediated by DR4 in Pancreatic Tumor Cells despite the Expression of Functional DR5. *J. Mol. Med.* **2010**, *88*, 729–740.
- (37) Kischkel, F. C.; Lawrence, D. A.; Chuntharapai, A.; Schow, P.; Kim, K. J.; Ashkenazi, A. Apo2L/TRAIL-Dependent Recruitment of Endogenous FADD and Caspase-8 to Death Receptors 4 and 5. *Immunity* **2000**, *12*, 611–620.
- (38) Wang, Y.; Baars, I.; Fördös, F.; Högberg, B. Clustering of Death Receptor for Apoptosis Using Nanoscale Patterns of Peptides. *ACS Nano* **2021**, *15*, 9614–9626.
- (39) Rosetti, C. M.; Mangiarotti, A.; Wilke, N. Sizes of Lipid Domains: What Do We Know from Artificial Lipid Membranes? What Are the Possible Shared Features with Membrane Rafts in Cells? *Biochim. Biophys. Acta Biomembr.* **2017**, 1859, 789–802.
- (40) Cornell, C. E.; Mileant, A.; Thakkar, N.; Lee, K. K.; Keller, S. L. Direct Imaging of Liquid Domains in Membranes by Cryo-Electron Tomography. *Proc. Natl. Acad. Sci. U. S. A.* **2020**, *117*, 19713–19719.
- (41) Heberle, F. A.; Doktorova, M.; Scott, H. L.; Skinkle, A. D.; Waxham, M. N.; Levental, I. Direct Label-Free Imaging of Nanodomains in Biomimetic and Biological Membranes by Cryogenic Electron Microscopy. *Proc. Natl. Acad. Sci. U.S.A.* **2020**, *117*, 19943–19952.
- (42) Zakaria, A. B.; Picaud, F.; Rattier, T.; Pudlo, M.; Saviot, L.; Chassagnon, R.; Lherminier, J.; Gharbi, T.; Micheau, O.; Herlem, G. Nanovectorization of TRAIL with Single Wall Carbon Nanotubes Enhances Tumor Cell Killing. *Nano Lett.* **2015**, *15*, 891–895.
- (43) Mitchell, M. J.; Webster, J.; Chung, A.; Guimarães, P. P. G.; Khan, O. F.; Langer, R. Polymeric Mechanical Amplifiers of Immune Cytokine-Mediated Apoptosis. *Nat. Commun.* **2017**, *8*, 14179.
- (44) Mitchell, M. J.; Wayne, E.; Rana, K.; Schaffer, C. B.; King, M. R. TRAIL-Coated Leukocytes That Kill Cancer Cells in the Circulation. *Proc. Natl. Acad. Sci. U. S. A.* **2014**, *111*, 930–935.
- (45) Jyotsana, N.; Zhang, Z.; Himmel, L. E.; Yu, F.; King, M. R. Minimal Dosing of Leukocyte Targeting TRAIL Decreases Triple-Negative Breast Cancer Metastasis Following Tumor Resection. *Sci. Adv.* **2019**, *5*, No. eaaw4197.
- (46) Ortiz-Otero, N.; Marshall, J. R.; Lash, B. W.; King, M. R. Platelet Mediated TRAIL Delivery for Efficiently Targeting Circulating Tumor Cells. *Nanoscale Adv.* **2020**, *2*, 3942–3953.
- (47) Brodszkij, E.; Westensee, I. N.; Bertelsen, M.; Gal, N.; Boesen, T.; Städler, B. Polymer–Lipid Hybrid Vesicles and Their Interaction with HepG2 Cells. *Small* **2020**, *16*, 1906493.
- (48) Rideau, E.; Wurm, F. R.; Landfester, K. Membrane Engineering: Phase Separation in Polymeric Giant Vesicles. *Small* **2020**, *16*, 1905230.

- (49) Christian, D. A.; Tian, A.; Ellenbroek, W. G.; Levental, I.; Rajagopal, K.; Janmey, P. A.; Liu, A. J.; Baumgart, T.; Discher, D. E. Spotted Vesicles, Striped Micelles and Janus Assemblies Induced by Ligand Binding. *Nat. Mater.* 2009 810 2009, 8, 843–849.
- (50) Rinaldin, M.; Fonda, P.; Giomi, L.; Kraft, D. J. Geometric Pinning and Antimixing in Scaffolded Lipid Vesicles. *Nat. Commun.* **2020**, *11*, 4314.
- (51) Rabanel, J.-M.; Adibnia, V.; Tehrani, S. F.; Sanche, S.; Hildgen, P.; Banquy, X.; Ramassamy, C. Nanoparticle Heterogeneity: An Emerging Structural Parameter Influencing Particle Fate in Biological Media? *Nanoscale* **2019**, *11*, 383–406.
- (52) Kern, N.; Dong, R.; Douglas, S. M.; Vale, R. D.; Morrissey, M. A. Tight Nanoscale Clustering of Fcγ Receptors Using DNA Origami Promotes Phagocytosis. *Elife* **2021**, *10*, 1–29.
- (53) Perica, K.; Tu, A.; Richter, A.; Bieler, J. G.; Edidin, M.; Schneck, J. P. Magnetic Field-Induced T Cell Receptor Clustering by Nanoparticles Enhances T Cell Activation and Stimulates Antitumor Activity. *ACS Nano* **2014**, *8*, 2252–2260.
- (54) Gonda, A.; Kabagwira, J.; Senthil, G. N.; Wall, N. R. Internalization of Exosomes through Receptor-Mediated Endocytosis. *Mol. Cancer Res.* **2019**, *17*, 337–347.
- (55) Moody, P. R.; Sayers, E. J.; Magnusson, J. P.; Alexander, C.; Borri, P.; Watson, P.; Jones, A. T. Receptor Crosslinking: A General Method to Trigger Internalization and Lysosomal Targeting of Therapeutic Receptor:Ligand Complexes. *Mol. Ther.* **2015**, 23, 1888–1808

